Journal of Solid State Chemistry **146,** 184–188 (1999)
Article ID jssc.1999.8329, available online at http://www.idealibrary.com on IDEAL®

State of Manganese Atoms during the Mechanochemical Synthesis of $LiMn_2O_4$

N. V. Kosova,*,[1] I. P. Asanov,† E. T. Devyatkina,* and E. G. Avvakumov*

*Institute of Solid State Chemistry and Mechanochemistry, Siberian Branch of RAS, ul.Kutateladze, 18, Novosibirsk 630128, Russia; and
†Institute of Inorganic Chemistry, Siberian Branch of RAS, pr.Lavrent'eva, 3, Novosibirsk 630090, Russia

Received November 17, 1998; in revised form April 1, 1999; accepted April 12, 1999

It has been established using X-ray photoelectron spectroscopy in combination with other physical methods that the initial stages of mechanochemical synthesis of $LiMn_2O_4$ in mixtures of MnO_2 with LiOH and Li_2CO_3 are considerably different. In the first case the "smearing" of LiOH, having a flaky structure, on the surface of MnO_2 and the formation of an amorphous layer take place. The reaction is accompanied by a redox process, with the participation of OH groups and Mn^{4+} ions and with diffusion of lithium ions to the interior of the particles, and is completed by formation of Li–O–Mn bonds. No change in the valence state of manganese was detected, in Li_2CO_3, only brittle fracture was observed. Formation of defect spinel-like $Li_2O \cdot yMnO_2$ ($2.5 \leq y \leq 4$) on the surface is proposed. © 1999 Academic Press

INTRODUCTION

Lithium–manganese spinels are of interest as prospective cathode materials for chemical current sources (1, 2). Development of new methods for their synthesis is a very urgent problem (3). One of the promising methods is a soft mechanochemical synthesis realized on the basis of compounds with hydroxyl groups (4). It allows the products to be synthesized under soft conditions either directly during mechanical activation or by preliminary activation followed by heat treatment at relatively low temperatures. The nature of the intermediate states formed during the mechanical activation is an important factor determining the properties of the final product. X-ray photoelectron spectroscopy in combination with other physical methods was found to be very useful for the investigation of the mechanism of mechanochemical reactions.

The aim of the present work is to study the initial stages of the mechanochemical synthesis of $LiMn_2O_4$ in the mixtures of β-MnO_2 with LiOH and Li_2CO_3.

EXPERIMENTAL

β-MnO_2 (Faradaizer), Li_2CO_3, and LiOH ("pure for analysis") were used as the initial reagents. LiOH was prepared from $LiOH \cdot H_2O$ by heating at 350°C.

Mechanical activation (MA) was carried out in an EI-2/150 activator with corundum jars and balls (5 mm, 660 revolutions/min). The mass ratio of material and balls was 1/40. Two series of samples were explored: mixtures of MnO_2 with LiOH and Li_2CO_3. The molar ratio Li/Mn was equal to 1/2.

The study of the composition and properties of the products was performed using X-ray photoelectron spectroscopy (XPS) combined with X-ray powder diffraction and IR spectroscopy, incorporating also the results of ^1H and ^7Li NMR received earlier (5).

The XPS study was carried out employing a VG Microtech photoelectron spectrometer using Mg$K\alpha$ X-ray irradiation (1253.6 eV) at room temperature. The pass energy of the electron analyzer was 20 eV, with the Ag $3d_{5/2}$ linewidth being 1.0 eV. The vacuum in the spectrometer was 10^{-6} Pa. Binding energies were calibrated relative to the C 1s peak (285.0 eV) from hydrocarbons adsorbed on the surface of the samples. The surface concentration ratios Li/Mn and O/Mn were calculated from the area ratios of the Mn 2p/O 1s and Mn 3p/Li 1s lines relative to $LiMn_2O_4$ (Merck) as a standard sample. For the XPS investigation the activated samples were pressed in pellets immediately after MA and hermetically packed into polyethlylene containers. The containers were opened just before inserting the samples into the preparation chamber of the spectrometer, with the surface of the pellets being scraped off.

X-ray analysis was made with a DRON-3.0 diffractometer (Cu$K\alpha$ irradiation). IR spectra were recorded on an IR spectrometer (Specord-75, pellets with KBr).

RESULTS AND DISCUSSION

Mixtures of MnO_2 with LiOH and Li_2CO_3 mechanically activated for 1 and 10 min were investigated. No substantial

[1] To whom correspondence should be addressed. Fax: +7 3832 322847. E-mail: kosova@solid.nsk.su.

0022-4596/99 $30.00

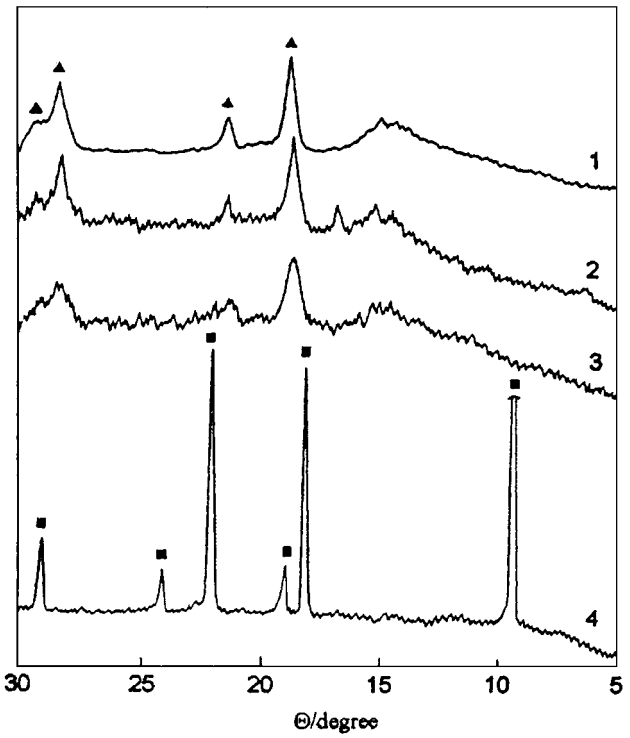

FIG. 1. X-ray patterns of initial and activated samples: (1) MnO_2; (2) LiOH + MnO_2, MA 1 min; (3) LiOH + MnO_2, MA 10 min; (4) same as (3) after heating at 800°C. ▲, MnO_2; ■, $LiMn_2O_4$.

chemical interaction between the initial compounds was observed from the X-ray data (Fig. 1). On the X-ray patterns one can see slightly broader and less intensive reflections of MnO_2. The peaks of the initial Li-containing compounds are present at the background level, due to the smaller X-ray scattering of lithium than of manganese atoms and due to the decreasing particle size and amorphization. No new crystal phase is observed.

By contrast, IR and NMR data (5) are indicative of some changes in the activated mixtures of MnO_2 and LiOH. In the IR spectra, the stretching vibrations of isolated OH groups disappear, but a broad asymmetric band, characteristic of OH groups with strong hydrogen bonds, appears in the region 3200–3600 cm^{-1} (Fig. 2).

A decrease in the second moment value, corresponding to the total proton concentration, was observed as a function of MA time in the ^1H NMR spectra of the mixture of MnO_2 and LiOH (5). The linewidth is approximately doubled in a stronger magnetic field. This fact points to the close proximity between hydrogen atoms contained in OH groups and paramagnetic manganese ions broadening the NMR spectra proportionally to the field strength. This could be a result of insertion of OH^- ions into the crystal lattice of β-MnO_2 and the formation of γ-MnO_2 (6). This modification of manganese dioxide contains OH groups, structurally similar to a spinel. However, the reflections of γ-MnO_2 are absent from the X-ray diffraction patterns, possibly due to the weak crystallization of the resulting product.

The ^7Li NMR spectra of the activated mixtures of MnO_2 with LiOH and Li_2CO_3 are considerably different. In the first case, strong shifts to weaker magnetic fields are observed. This behavior is characteristic of a paramagnet, while lithium hydroxide is diamagnetic. In addition, the value of the shift increases with the time of activation (see Table 1) and does not coincide with that in the final paramagnetic crystalline product, $LiMn_2O_4$ [according to (5), (7)].

X-ray photoelectron spectra of the activated samples and the initial compounds, as well as of $LiMn_2O_4$ (Merck) and Mn_2O_3, were recorded. Mn_2O_3 was prepared by heating MnO_2 at 700°C in air.

The Mn 2*p*, Mn 3*p*, Mn 3*s*, Li 1*s*, O 1*s*, and C 1*s* core-level spectra were determined. The binding energies are listed in Table 2 and the compositions of the surface layers in Table 3. Figures 3 and 4 display the spectra of the Mn 3*s* and O 1*s* levels.

We first discuss the chemical shifts in the spectra of the standard samples. The maximum position of the Mn $2p_{3/2}$ line is 0.5 eV higher in MnO_2 than in Mn_2O_3. Correspondingly, the binding energy of the O 1*s* level in MnO_2 is less

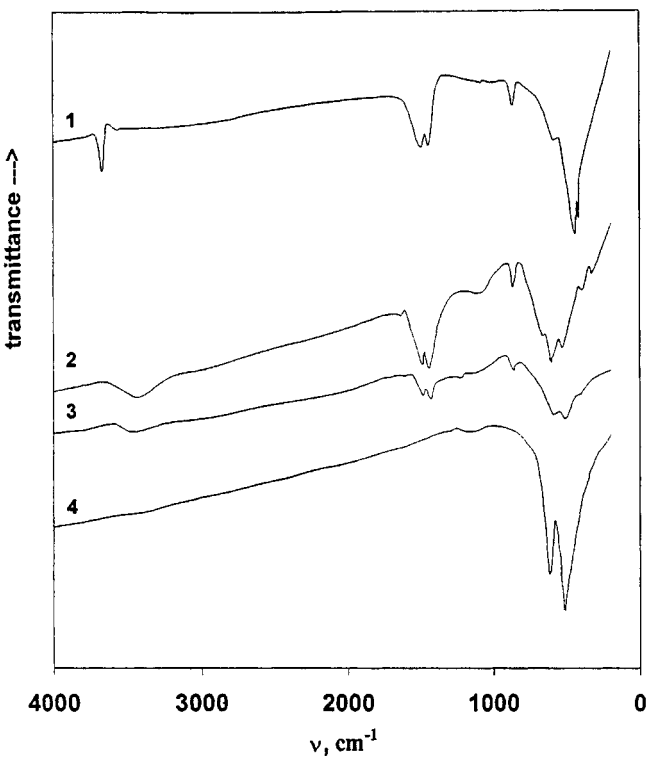

FIG. 2. IR spectra of initial and activated samples: (1) LiOH; (2) LiOH + MnO_2, MA 1 min; (3) LiOH + MnO_2, MA 10 min; (4) same as (3) after heating at 800°C.

TABLE 1
Values of Nuclear Quadrupolar Constants (eQq/h), Gravity Center Shifts (δ), and Half-Widths ($\Delta\omega$) of Lithium Spectra of the Initial and Activated Samples (5)

Sample	eQq/h (kHz)	δ (ppm)	$\Delta\omega$ (ppm)
LiOH	50	0 ± 10	790 ± 40
$LiOH + MnO_2$, MA 1 min	—	50 ± 50	910 ± 40
$LiOH + MnO_2$, MA 10 min	—	800 ± 50	1500 ± 40
Li_2CO_3	63	0 ± 10	560 ± 40
$Li_2CO_3 + MnO_2$			
MA 1 min	90	-60 ± 50	560 ± 40
MA 10 min	90	-80 ± 50	830 ± 40
$LiMn_2O_4$	0	470 ± 50	790 ± 40

than in Mn_2O_3 by 0.4 eV. This is connected to the increasing degree of Mn–O bond ionicity in MnO_2. Further, the value of the Mn 3*s* multiplet splitting [Δ(Mn 3*s*)], proportional to the number of unpaired 3*d* electrons, is informative, as well (8). For Mn_2O_3 (spin $S = 2$) this value is 5.4 eV and for MnO_2 ($S = 3/2$) it is 4.7 eV. In $LiMn_2O_4$ the Mn 3*s* line splitting practically coincides with that in MnO_2 (Fig. 3). This indicates that surface manganese atoms of the spinel are predominantly in the Mn^{4+} state. When going from MnO_2 to $LiMn_2O_4$, a simultaneous increases in the binding energies of Mn and O core levels are observed. The Li 1*s* line is localized close to the Mn 3*p* spectrum. The position of its maximum (55.0 eV) coincides with that in LiOH and Li_2CO_3. This suggests that lithium atoms are in the Li^+ oxidation state. In the O 1*s* spectra of all manganese oxides a weak broad component is observed in addition to a main line. The binding energy of this component is higher by $\sim$1.6 eV than that of the main component. We suggest that the main line originates from oxygen atoms in the compounds under study, whereas the additional component is associated largely with water absorbed on the surface (Fig. 4). Note that the binding energy of this peak coincides with the binding energy of the O 1*s* level in LiOH and Li_2CO_3.

TABLE 2
Binding Energies (eV) of Core-Level Spectra in the Initial and Activated Samples

Sample	Mn $2p_{3/2}$	O 1*s*	Δ(Mn 3*s*)[a]	Δ(Mn $2p_{3/2}$ − O 1*s*)[b]
MnO_2	643.0	530.0	4.7	113.0
Mn_2O_3	642.5	530.4	5.4	112.1
$LiMn_2O_4$	643.3	530.5	4.8	112.8
LiOH		531.7		
Li_2CO_3		531.5		
$LiOH + MnO_2$,				
1 min MA			4.7	112.7
10 min MA			5.0	112.7
10 min MA and after heating at 800°C	643.0	530.3	5.0	112.7
$Li_2CO_3 + MnO_2$,				
1 min MA			4.6	112.8
10 min MA			4.6	112.9
10 min MA and after heating at 800°C	643.4	530.6	4.7	112.8

[a] Value of Mn 3*s* level multiplet splitting.
[b] Difference between the binding energies of core levels of manganese and oxygen atoms, participating in the chemical bond.

TABLE 3
Changing of Surface Layer Content of Activated Samples

Sample	O/Mn	Li/Mn
$LiOH + MnO_2$		
1 min MA	3.0	3.2
10 min MA	2.5	1.6
10 min MA and after heating at 800°C	1.4	1.8
$Li_2CO_3 + MnO_2$		
1 min MA	2.1	0.8
10 min MA	2.5	2.0
10 min MA and after heating at 800°C	1.3	1.7

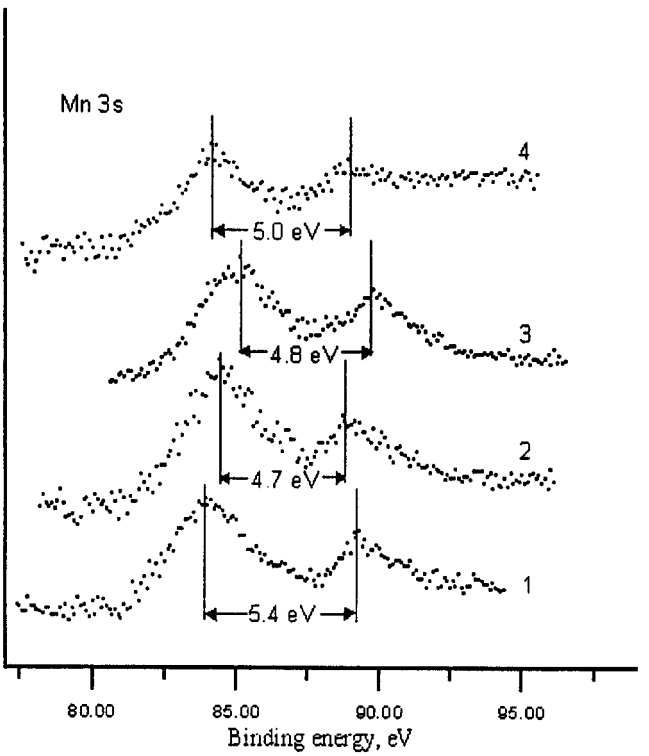

FIG. 3. X-ray photoelectron spectra of Mn 3*s* level of initial and activated samples: (1) Mn_2O_3; (2) MnO_2; (3) $LiMn_2O_4$; (4) $LiOH + MnO_2$, MA 10 min and after heating at 800°C.

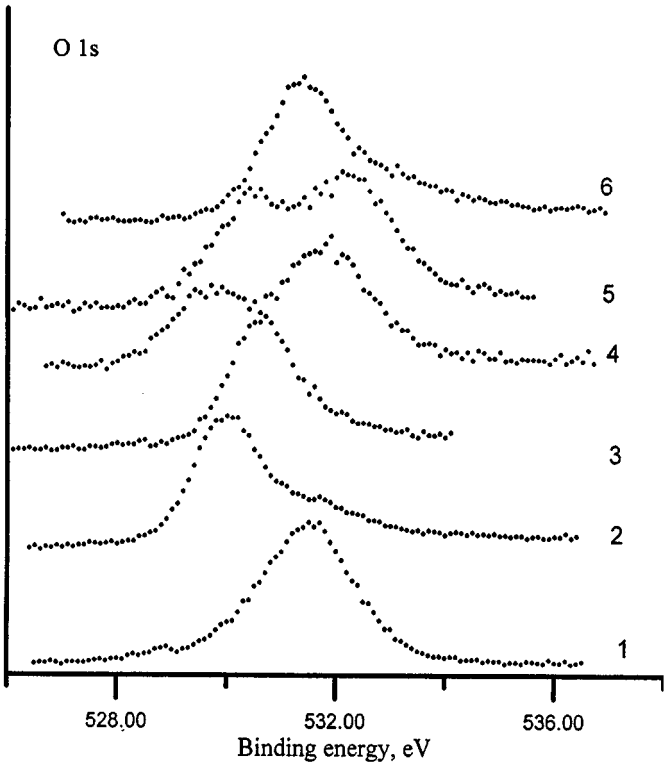

FIG. 4. X-ray photoelectron spectra of O 1*s* level of initial and activated samples: (1) LiOH; (2) MnO_2; (3) $LiMn_2O_4$; (4) LiOH + MnO_2; MA 1 min; (5) LiOH + MnO_2, MA 10 min; (6) same as (5) after heating at 800°C.

When interpreting the XPS shifts in activated samples, it is necessary to take into account the effect of differential charging. In this connection the calculation of differences in binding energy is useful. One such parameter is the Mn 3*s* splitting. The difference between the core-level binding energies of atoms participating in bonding is usable for characterization of the chemical bond. For instance, the differences between the binding energies of the Mn $2p_{3/2}$ and O 1*s* levels in MnO_2 and Mn_2O_3 are 113.0 and 112.1 eV, respectively. In $LiMn_2O_4$ this difference is 112.8 eV close to that in MnO_2.

We next discuss the spectrum changes occurring under MA of MnO_2 with LiOH. The Mn 3*s* multiplet splitting in the sample activated for 1 min shows that the surface manganese atoms are in the same valence state as in the initial MnO_2. After 10 min of MA, the degree of splitting increases to 5.0 eV. This indicates that the manganese atoms in the sample are in two valence states: Mn(+3) and Mn(+4). The difference between the Mn $2p_{3/2}$ and O 1*s* binding energies does not depend on the length of activation and is equal to 112.7 eV.

The O 1*s* level spectra show that the hydroxide and carboxide groups dominate the surface after 1 min of activation. But after 10 min, oxygen atoms directly linked to manganese atoms prevail; in this case, an increase occurs in the Mn/O concentration ratio on the surface. According to the ^1H NMR data, protons remain in the system; one may suppose that they have diffused to the interior of the particles.

The Li/Mn ratio on the surface of particles in the MnO_2–LiOH mixture activated for 1 min is twice as large as the value in the mixture after 10 min of activation. But after 10 min of MA, the Li/Mn ratio is still 1.6 times larger than in the Merck spinel (see Table 3); i.e., the surface layer of particles in activated mixtures is enriched by amorphous LiOH.

Based on the above data it is possible to reconstruct the changes occurring on the surface of MnO_2–LiOH mixtures. During the initial stage of MA, a "smearing" of LiOH, having a flaky structure, occurs on the surface of MnO_2 particles, and an amorphous layer forms. This fact is confirmed by X-ray data. As follows from the IR and ^1H NMR data, the hydroxyl groups are thereby bound by hydrogen bonds to water molecules and locate near paramagnetic manganese ions. Amorphous γ-MnO_2 may form. The subsequent chemical interaction is associated with an electron transfer from OH groups of LiOH to the Mn^{4+} ions, partially reducing them to Mn^{3+}.

In summary, the process can be represented by the redox equation

$$4LiOH + 8MnO_2 = 4LiMn^{3+}Mn^{4+}O_4 + 2H_2O + O_2,$$

or in compact notation,

$$4OH^- - 4e = 2H_2O + O_2,$$

$$4Mn^{4+} + 4e = 4Mn^{3+}.$$

At the same time, lithium ions diffuse to the interior of the particle, resulting in a decrease in the lithium concentration in the surface layer.

The appearance of the strong paramagnetic shift in the ^7Li NMR spectra of the activated mixtures of MnO_2 with LiOH is connected to a spin density transfer on lithium atoms and, in our opinion, is induced by the appearance of Mn^{3+} ions and by *s*–*d* band overlap. These processes, finally, bring about formation of Li–O–Mn bonds.

A different picture is observed when milling MnO_2 and Li_2CO_3. The value of Δ(Mn 3*s*) does not depend on activation time and is equal to 4.6 eV, indicating that the valence state of manganese atoms remains close to that in MnO_2. The difference between the binding energies of the Mn $2p_{3/2}$ and O 1*s* levels is unchanged and equal to 112.8 eV. On an increase in activation time, the Mn/Li ratio decreases. Accordingly, the component with smaller binding energy (from MnO_2) dominates the O 1*s* spectrum initially; its intensity

further decreases and the contribution from oxygen atoms of hydroxide and carboxide groups increases.

Based on these data, it is possible to conclude that no observable chemical interaction occurs between MnO_2 and Li_2CO_3 during MA. As a consequence, the change in XPS line intensity is determined by the ratio of the surface areas of the components of the mixture; i.e., the signal depends on the shape and change in size of particles during milling [so-called "size" effect (9)].

Heating the activated mixtures to 800°C brings about the formation of Li–Mn–O spinel (Fig. 1). According to XPS data, the value of Δ(Mn 3*s*) in the annealed mixture of MnO_2 and LiOH is unchanged at 5.0 eV, indicating that manganese atoms are in two oxidation states (3+ and 4+). The difference between the binding energies of the Mn $3p_{3/2}$ and O 1*s* levels (112.7 eV) is also the same. The intensity ratios Li/Mn and O/Mn, respectively, are 1.8 and 1.4 times larger than in the Merck spinel. In mixtures with Li_2CO_3 the valence state after heating is also the same: all manganese atoms are in the 4+ state [Δ(Mn 3*s*) = 4.6 eV]. The surface composition is close to that of the spinel obtained after heating the mixture containing LiOH (Table 3). In our opinion, the results can be explained by the formation of defect spinel line $Li_2O \cdot yMnO_2$ ($2.5 \leq y \leq 4$) by substituting some of the manganese atoms in octahedral position for lithium atoms (10). This conclusion is in accord with the data on the study of $LiMn_2O_4$ by X-ray absorption spectroscopy (11).

Thus, the differences in the valence states of manganese atoms are determined by the presence or absence of hydroxide groups in the initial mixture and by their participation in redox processes.

The reaction with Li_2CO_3 probably proceeds according to the equation

$$Li_2CO_3 + yMnO_2 = Li_2O \cdot MnO_2 + CO_2$$

in which the redox stage is absent.

CONCLUSIONS

Our investigations demonstrate that the processes during the initial stages of MA in mixtures of MnO_2 with LiOH and Li_2CO_3 are different in nature. The interaction of MnO_2 with LiOH begins with "smearing" of LiOH, having a flaky structure, on the surface of MnO_2. The reaction is accompanied by a redox process, with the participation of hydroxide groups and Mn^{4+} ions and with diffusion of lithium ions to the interior of the particles. The formation of Li–O–Mn bonds thereby begins, so that a spinel is formed in the course of the subsequent heating.

In the case of Li_2CO_3, no redox process was observed during MA; only brittle fracture occurred. The increased content of surface lithium atoms after 10 min of activation and in the final product in comparison with the Merck spinel can be explained by the formation of a defect spinel like $Li_2O \cdot yMnO_2$ ($2.5 \leq y \leq 4$) on the surface. These spinels have cubic structure, but the lithium and oxygen contents are higher than in $LiMn_2O_4$, and all manganese atoms are in the 4+ valence state.

It is worth noting that the reaction between MnO_2 and LiOH represents a new, more complex type of reaction induced by soft mechanochemical synthesis. Aside from an acid–base interaction, with the participation of proton-containing groups, a redox process takes place that is connected to an electron transfer from the OH group to the transition metal atom.

ACKNOWLEDGMENT

The authors thank the Russian Foundation for Basic Research for financial support (Project 97-03-33524a).

REFERENCES

1. J. M. Tarascon, E. Wang, F. K. Shokoohi, *et al*., *J. Electrochem. Soc.* **138,** 2859 (1991).
2. M. M. Thackeray, A. de Kock, M. H. Rossouw, D. C. Liles, *et al*., *J. Electrochem. Soc.* **139,** 363 (1992).
3. V. S. Pervov, I. V. Kedrinskii, and E. V. Machonina, *Neorg. Mater.* **33,** 1031 (1997).
4. E. G. Avvakumov, N. V. Kosova, *Chem. Rev.* **23,** (Pt. 2), 285 (1998), Harwood, Reading, U.K.
5. N. V. Kosova, S. G. Kozlova, S. P. Gabuda, and E. G. Avvakumov. *Dokl. Ross. Acad. Nauk* **362,** 493 (1998).
6. G. P. Ereiskaya, O. N. Khodarev, V. I. Ezikian, and V. G. Kalaida, *Neorg. Mater*, **32,** 1127 (1996).
7. K. R. Morgan, S. Collier, G. Burns, and K. Ooi, *J. Chem. Soc. Chem. Commun*., **14,** 1719 (1994).
8. D. G. Kellerman, V. S. Gorshkov, V. G. Zubkov, V. A. Perelyaev, V. R. Galakhov, E. Z. Kurmaev, St. Uhlenbrock, and M. Neumann, *Zh. Neorg. Khim.* **42,** 1012 (1997).
9. Kh. M. Minachev, G. V. Antoshin, and E. S. Shpiro, "Photoelectronaya Spectroscopiya i ejo Primenenije v Katalize" ["Photoelectron Spectroscopy and Its Application in Catalysis"]. Nauka, Moscow, 1981. [In Russian.]
10. M. M. Thackeray, A. de Kock, and W. I. F. David, *Mater. Res. Bull.* **28,** 1041 (1993).
11. R. S. Liu, L. Y. Jang, J. M. Chen, Y. D. Tsai, Y. D. Hwang, and R. G. Liu, *J. Solid State Chem.* **128,** 326 (1997).